Published online 11 June 2022

Nucleic Acids Research, 2022, Vol. 50, No. 11 ***6497–6510***
https://doi.org/10.1093/nar/gkac437

The domains of yeast eIF4G, eIF4E and the cap fine-tune eIF4A activities through an intricate network of stimulatory and inhibitory effects

Linda Krause, Florian Willing, Alexandra Zoi Andreou and Dagmar Klostermeier*

Institute for Physical Chemistry, University of Muenster, Corrensstrasse 30, 48149 Muenster, Germany

Received November 05, 2021; Revised April 19, 2022; Editorial Decision May 05, 2022; Accepted May 23, 2022

ABSTRACT

Translation initiation in eukaryotes starts with the recognition of the mRNA 5′-cap by eIF4F, a hetero-trimeric complex of eIF4E, the cap-binding protein, eIF4A, a DEAD-box helicase, and eIF4G, a scaffold protein. eIF4G comprises eIF4E- and eIF4A-binding domains (4E-BD, 4A-BD) and three RNA-binding regions (RNA1–RNA3), and interacts with eIF4A, eIF4E, and with the mRNA. Within the eIF4F complex, the helicase activity of eIF4A is increased. We showed previously that RNA3 of eIF4G is important for the stimulation of the eIF4A conformational cycle and its ATPase and helicase activities. Here, we dissect the interplay between the eIF4G domains and the role of the eIF4E/cap interaction in eIF4A activation. We show that RNA2 leads to an increase in the fraction of eIF4A in the closed state, an increased RNA affinity, and faster RNA unwinding. This stimulatory effect is partially reduced when the 4E-BD is present. eIF4E binding to the 4E-BD then further inhibits the helicase activity and closing of eIF4A, but does not affect the RNA-stimulated ATPase activity of eIF4A. The 5′-cap renders the functional interaction of mRNA with eIF4A less efficient. Overall, the activity of eIF4A at the 5′-cap is thus fine-tuned by a delicately balanced network of stimulatory and inhibitory interactions.

INTRODUCTION

The initiation of translation on eukaryotic mRNAs depends on a number of translation initiation factors (eIFs). These factors cooperate in recognizing the 5′-end of the mRNA by binding to its 5′-cap, in recruitment of the 40S ribosomal subunit to the 5′-end, and in scanning of the pre-initiation complex (PIC) along the 5′-untranslated region (5′-UTR) to the AUG start codon. When the start codon is reached, the 60S ribosomal subunit is recruited, and protein synthesis commences (reviewed in (1–4)).

The initial recognition of the mRNA 5′-end involves the translation factor eIF4F, a hetero-trimeric complex formed by the assembly of eIF4A, eIF4E, and eIF4G (5,6). eIF4E is the cap-binding protein that specifically binds to the 5′-cap structure (7,8). eIF4E also interacts with the scaffold protein eIF4G (5,9,10). eIF4G in turn binds to eIF4A (5,11), a DEAD-box helicase that has been implicated in the unwinding of double-stranded regions in the 5′-UTR that might otherwise interfere with PIC recruitment and scanning (12). eIF4A is a much more efficient helicase when part of the eIF4F complex (13–15). eIF4B, and in mammals eIF4H, are RNA binding proteins that further stimulate eIF4A activities in translation initiation (15–22).

The cellular levels of translation initiation factors are regulated according to the physiological conditions (23,24); in humans, their dysregulation is linked to cancer (25). The concentrations of individual translation initiation factors in yeast have been determined under standard growth conditions (26). These studies revealed that eIF4E and eIF4A are present in excess over eIF4G (2 μM), making eIF4G the limiting factor for eIF4F formation. The affinities of eIF4G for eIF4A and eIF4E are in the low micromolar and nanomolar range, respectively (27–29). Thus, under cellular conditions, eIF4G is present almost exclusively as part of the eIF4F complex. The eIF4A/4G complex, although not significantly populated in equilibrium, might be populated transiently as an intermediate during eIF4F assembly (29). Notably, most of eIF4A and eIF4E is left without binding partners, available for other tasks outside eIF4F and independent of the 5′-cap. While eIF4E also participates in mRNA export from the nucleus (30), the cellular function of free eIF4A is less clear (31).

The basic interaction principles within the eIF4F complex can be gleaned from crystal structures and NMR analyses of yeast and human eIF4E in the apo form and in complex with the 5′-cap, and structures of *Saccharomyces cerevisiae* and human eIF4E/4G and eIF4A/4G complexes (9–11,32–36). The interaction between eIF4E and eIF4G is

*To whom correspondence should be addressed. Tel: +49 251 8323421: Email: dagmar.klostermeier@uni-muenster.de

largely conserved between yeast and humans, despite the substantially different domain organizations of yeast and human eIF4G. The eIF4G/4E complex is formed through the interaction of eIF4E with the eIF4E-binding domain (4E-BD) of eIF4G (10,37,38) (Figure 1A). In humans, a non-canonical loop of eIF4G contacts the lateral side of eIF4E; this loop is absent in yeast eIF4G (10). The interaction of eIF4E with the 4E-BD of 4G leads to an increase in the affinity of eIF4E for the 5′-cap (27,39,40). In yeast, this increase in affinity has been ascribed to an allosteric effect of 4E-BD binding to the surface distal from the cap-binding site of eIF4E (9). For human eIF4E, the affinity is increased through binding of multiple RNA-binding domains of eIF4G to mRNA regions outside the cap, which anchors eIF4E on the mRNA (41). Notably, the interaction of yeast eIF4E with the 5′-cap varies tremendously from mRNA to mRNA, with association rate constants covering more than an order of magnitude (42). The velocity of association is anti-correlated with the propensity of the mRNA to form secondary structures (42).

The interaction of eIF4A with eIF4G is mediated by the eIF4A-binding domain (4A-BD) of 4G (Figure 1A), both in yeast and humans (43,44). Human eIF4G contains a second eIF4A binding site (43,45–47). Both sites are crucial for translation initiation (45), but only the site conserved between humans and yeast is involved in the stimulation of the eIF4A ATPase activity (46). Through this site, eIF4G binds to both RecA-like domains of eIF4A and pre-aligns them in a half-open state (11,28,32,35), poised for formation of the closed state that causes duplex destabilization and RNA unwinding (11,28). Both human and yeast eIF4G also contain several RNA-binding regions that mediate interactions with the mRNA (14,48). Yeast eIF4G contains three regions involved in RNA binding, termed RNA1 to RNA3 (Figure 1A). The most N-terminal region, RNA1, has been implicated in the assembly of the eIF4F/mRNA complex, whereas RNA2, located between the 4E-BD and the 4A-BD, and RNA3, located in the C-terminal region of eIF4G, are thought to play a role in downstream processes such as PIC attachment and scanning (49). Deletion of RNA1 leads to a moderate, approx. two-fold decrease in the rate constant for RNA unwinding by eIF4F, whereas deletion of RNA2 or RNA3 reduces the rate constant for unwinding by 10–15-fold, and abrogates the preference of eIF4F for RNA substrates with a 5′-single-stranded tail (14).

The DEAD-box helicase eIF4A and eIF4E do not interact directly, but affect one another through their association with eIF4G and the mRNA: Yeast eIF4A accelerates the association of eIF4E with the cap (42). This effect correlates with the propensity of the mRNA for structure formation, and could be an indirect effect caused by the helicase function of eIF4A. In turn, human eIF4E stimulates RNA unwinding by eIF4A within the eIF4F complex (13).

Despite a large body of biochemical data (e.g. (13–18,21,28,44,50–57)), the regulatory interplay between the different factors and their constituent domains in cap-dependent and -independent interactions with mRNA is not very well understood. We have previously shown that the RNA3 domain of eIF4G contributes to the stimulation of the ATPase activity of eIF4A by increasing k_{cat} and decreasing $K_{1/2}$ for RNA, and to the promotion of eIF4A closing by eIF4G (18). Here, we analyze the interplay between RNA2 and the 4E- and 4A-BDs of eIF4G in eIF4A activation, and dissect the role of eIF4E and the 5′-cap for eIF4A activities. We show that the presence of RNA2 is correlated with an increase in the fraction of eIF4A in the closed state, an increased RNA affinity, and faster RNA unwinding. This stimulatory effect is partially reduced when the 4E-BD is present. eIF4E and the 5′-cap show independent effects on eIF4A: eIF4E binding to eIF4A/4G is associated with a reduced unwinding activity and a smaller fraction of eIF4A in the closed state, but does not alter the eIF4A ATPase activity and its functional interaction with RNA. The 5′-cap has little effect on RNA unwinding or ATP hydrolysis by eIF4A, but leads to an increase in the $K_{1/2}$ value for RNA, indicating that the functional interaction of capped RNA with eIF4A is less efficient. Overall, the activity of eIF4A at the 5′-cap is fine-tuned by a delicately balanced network of stimulatory and inhibitory effects.

MATERIALS AND METHODS

Protein production and purification

Yeast eIF4A, N-terminally biotinylated eIF4A_Q186C/G370C (bio-eIF4A), eIF4E, and the eIF4G variants eIF4G-A, -RA, -R*A and -ERA (Figure 1A) were produced recombinantly in *Escherichia coli*. eIF4G-A (amino acids 572–952) comprises the middle and C-terminal domains of eIF4G, i.e. the eIF4A binding domain (4A-BD) and RNA3. It was previously termed eIF4G-MC (16–18,51), but now renamed to eIF4G-A to indicate the presence of the 4A-BD. eIF4G-RA and -R*A (amino acids 492–952) both comprise RNA2, the 4A-BD and RNA3; in eIF4G-R*A, twelve arginines within RNA2 are replaced by alanines (in positions 493, 497, 504, 509, 514, 519, 523, 528, 529, 532, 537 and 538), which abrogates RNA binding (48). eIF4G-ERA (amino acids 380–952) comprises the eIF4E-binding domain (4E-BD), the second of three RNA-binding domains (RNA2), the 4A-BD, and RNA3. eIF4A, eIF4A-bio, eIF4B and eIF4G-A were purified as described (17,18). eIF4G-ERA, -RA, and -R*A were overproduced in *E. coli* Rosetta (DE3) in 2YT medium at 37°C. Gene expression was induced with 0.1 mM isopropyl-β-D-thiogalactoside (IPTG) at an optical density at 600 nm (OD_{600}) of 0.6, and cell growth was continued overnight at 20°C. eIF4E was overproduced in *E. coli* BL21 (DE3) in LB medium. Gene expression was induced with 0.1 mM IPTG at $OD_{600} = 0.6$ and continued for 4 h at 37°C. Cells overproducing eIF4E, eIF4G-ERA, -RA, or R*A were harvested by centrifugation and resuspended in 50 mM Tris/HCl pH 7.5, 500 mM NaCl, 20 mM imidazole and 2 mM β-mercaptoethanol (β-ME) and disrupted in a microfluidizer. The supernatant was applied to a Ni^{2+}-NTA sepharose column (GE Healthcare, 10 ml), and eluted with the same buffer supplemented with 200 mM imidazole. The His_6-tag (eIF4E, eIF4G-RA, -R*A) or His_6-SUMO-tag (eIF4G-ERA) was cleaved with thrombin (eIF4E) or TEV protease (eIF4G-ERA, eIF4G-RA, eIF4G-R*A) during overnight dialysis against

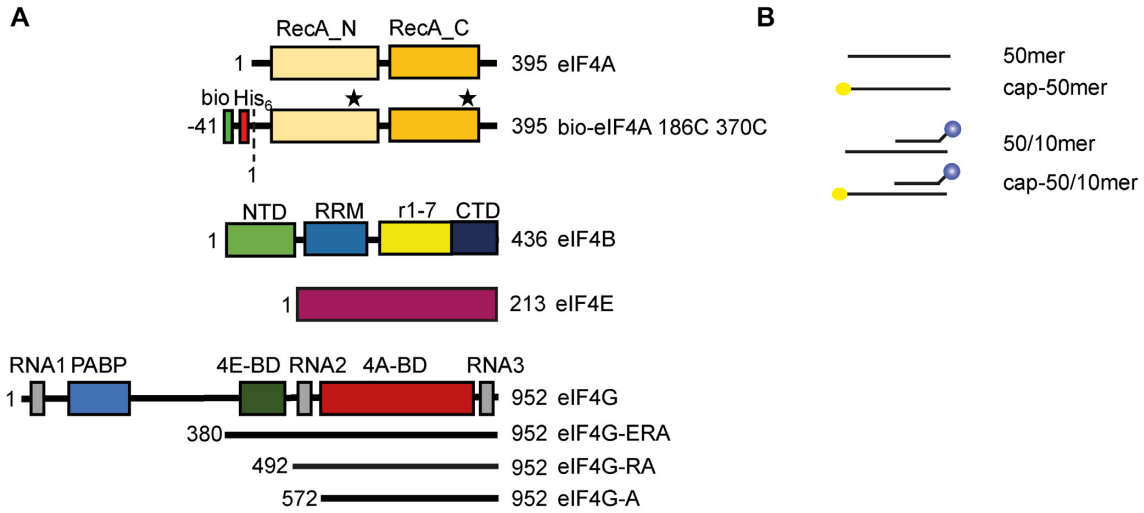

Figure 1. Translation initiation factors and RNA substrates used. (**A**) eIF4A, eIF4B, eIF4E and eIF4G constructs used in this work. eIF4G-ERA: deletion variant of eIF4G comprising amino acids 512–952; eIF4G-RA: deletion variant of eIF4G comprising amino acids 492–952; eIF4G-A: deletion variant of eIF4G comprising amino acids 572–952 (previously termed eIF4G-MC). eIF4G-R*A comprises the same domains as eIF4G-RA, but arginines 493, 497, 504, 509, 514, 519, 523, 528, 529, 532, 537 and 538 in RNA2 have been exchanged to alanines (48). Note that all eIF4G variants also contain the third, C-terminal RNA-binding region (RNA3) not reflected in their names. 4A-BD: eIF4A-binding domain; 4E-BD: eIF4E-binding domain; bio: biotinylation sequence; His_6: hexa-histidine tag; NTD, CTD: N-, C-terminal domain; PABP: poly-A-binding protein binding domain; r1-7: 7-repeats domain; RBD: RNA-binding domain; RecA_N, RecA_C: N- and C-terminal RecA domain; RNA2: second RNA-binding region of eIF4G; RNA3: third RNA-binding region of eIF4G; RRM: RNA recognition motif. The stars denote the cysteines C186 and C370 for donor/acceptor labeling of eIF4A. (**B**) RNAs used in this work. The blue sphere indicates the fluorescein attached to the 5′-end of the 10mer for fluorescence detection. The yellow sphere represents the 5′-cap. cap-50mer: capped 50mer.

50 mM Tris/HCl pH 7.5, 500 mM NaCl and 2 mM β-ME at 4°C. The tags and uncleaved fusion protein were removed in a second purification step on Ni^{2+}-NTA sepharose. The flowthrough was concentrated to < 5 mL and further purified on an S75 (eIF4E) or S200 (eIF4G-ERA, -RA, -R*A) size-exclusion column (120 ml, GE Healthcare) equilibrated with 50 mM Tris/HCl pH 7.5, 500 mM NaCl and 2 mM β-ME. eIF4G-ERA was further purified on a MonoQ ion-exchange column (1 ml, GE Healthcare) equilibrated in 50 mM Tris/HCl pH 7.5, 100 mM NaCl and 2 mM β-ME. After a washing step with 5 % buffer containing 50 mM Tris/HCl pH 7.5, 1 M NaCl, and 2 mM β-ME, 4G-ERA was eluted in a linear gradient from 5 to 20% of the high-salt buffer in 25 ml. Protein purity was >95% according to Coomassie-stained SDS-PAGE.

The plasmid for overproduction of the capping enzyme was provided by Remco Sprangers (University of Regensburg, Germany). The capping enzyme was produced and purified as described (58). The plasmid for overproduction of T7 RNA polymerase Y639F was provided by Roland K. Hartmann (University of Marburg, Germany). T7 RNA polymerase was produced and purified as described (59).

Pull-down assays

Interactions of eIF4G variants with eIF4A and eIF4E were tested in pull-down experiments using His_6-tagged eIF4E. To this end, 0.5 μM His_6-eIF4E were incubated with 2 μM eIF4A and 0.2 μM eIF4G in 40 mM Tris/HCl pH 7.5, 300 mM NaCl, 10 mM $MgCl_2$, 20 mM glycerol and 0.2 mM Tween20 on ice for 1 h. Complexes formed were isolated by incubation with 20 μl Ni^{2+}-NTA resin per 100 μl at 25°C for 1 h; the sample was constantly mixed during the incubation. The resin was precipitated by centrifugation (800 g, 30 s). As a control for unbound protein, 15 μl of the supernatant were removed. The resin was washed three times with 500 μl of 50 mM Tris/HCl pH 7.5, 500 mM NaCl, 20 mM imidazole, and 2 mM β-ME. Complexes were eluted with the same buffer supplemented with 200 mM imidazole, followed by centrifugation (800 g, 30 s). 15 μl of the supernatant were analysed by SDS-PAGE on 15 % acrylamide gels.

DNA and RNA oligonucleotides

50mer RNA (5′-GGG GAG AAA AAC AAA ACA AAA CAA AAC AAA ACU AGC ACC GUA AAG CAC GC; the sequence to which the 10mer to generate the double-stranded substrate binds is underlined) for unwinding assays was purchased HPLC-purified from Dharmacon, the complementary 10mer (5′-GCU UUA CGG U) and 10mer labeled with fluorescein at the 5′-end (5′-FAM-GCU UUA CGG U) were purchased HPLC-purified from Sigma. For capping purposes, ATPase activity assays, and single-molecule FRET experiments, the 50mer was produced by *in vitro*-transcription from a linear DNA template (5′-CAG AGA TGC ATA ATACGA CTC ACT ATA**G** GGG GAG AAA AAC AAA ACA AAA CAA AAC AAA ACT AGC ACC GTA AAG CAC GC; the T7 RNA polymerase binding site is underlined, the transcription start is highlighted in bold). The two DNA strands used to generate the DNA template *in vitro* transcription were purchased from Sigma and annealed by heating an equimolar mixture to 95°C for 1 min and slow cooling to room temperature.

In vitro transcription and capping of RNA

50 ng/μl DNA template were incubated with 0.01 volumes of T7 RNA polymerase and 0.12 U inorganic pyrophosphatase (ThermoFisher) in 40 mM HEPES/KOH pH 7.5, 2 mM dithiothreitol (DTT), 5 mM spermidine, 5% (v/v) dimethyl sulfoxide, 40 mM $MgCl_2$ and 4 mM NTPs (each) for 2 h at 37°C in 50 μl aliquots. After further addition of 1/75 volume of T7 RNA polymerase, the reaction was continued for 2 h at 37°C. Reactions were stopped with 45 mM EDTA. The RNA was precipitated by adding 1/10 volume of 3 M sodium acetate and 2.5 volumes of 100% ethanol at −20°C, and pelleted by centrifugation (21 000 g, 30 min, 4°C). The pellet was washed twice with 70% ethanol and dried. The RNA was dissolved in ddH_2O, and purified by electrophoresis on an 8 M urea polyacrylamide gel, and extracted from the gel by crush elution and precipitation.

For subsequent capping, 1 nmol of RNA was incubated in ddH_2O at 65°C for 10 min and stored at 4°C for 5 min. The capping reaction was carried out with 0.5 mM GTP, 0.1 mM *S*-adenosyl-methionine, and 1/10 volume of capping enzyme in 50 mM Tris/HCl pH 8.0, 5 mM KCl, 1 mM $MgCl_2$ and 1 mM DTT for 1 h at 37°C, followed by RNA precipitation.

RNA binding

Binding of eIF4G-A, -RA and R*A to the 50/10mer RNA was followed in fluorescence anisotropy titrations of the 50/10mer (formed by annealing the 50mer with the 5′-FAM-labeled 10mer) with the respective eIF4G variant in 30 mM HEPES/KOH, pH 7.5, 100 mM KOAc, 3 mM $Mg(OAc)_2$, and 2 mM DTT at 25°C in a Jobin-Yvon Fluoromax-4 spectrometer equipped with polarizers. Fluorescence was excited at 490 nm (3 nm bandwidth) and parallel and perpendicular components of the emission at 520 nm (6 nm bandwidth) were measured for 3 min to calculate the fluorescence anisotropy.

RNA unwinding

50 μM 50mer RNA or 30 μM capped 50mer RNA and 25 μM or 15 μM of 10mer-fluorescein RNA were annealed in 25 mM HEPES/KOH pH 7.5 by incubating for 2 min at 96°C, slow cooling down to room temperature and incubating on ice for 15 min. 500 nM of this double-stranded RNA were incubated with 5 μM of 10mer (as a trap) and 5 μM eIF4A in the presence and absence of 5 μM eIF4G, 5 μM eIF4E, 5 μM eIF4B and 3 mM ATP. Reactions were performed in 50 mM Tris/HCl pH 7.5, 80 mM KCl, 2.5 mM $MgCl_2$, 1 mM DTT and 1% (v/v) glycerol at 25°C. The reaction was stopped at different time points with 1% SDS, 50 mM DTT, 5% (v/v) glycerol, 0.05 mg/ml proteinase K. Substrate and product were separated by native gel electrophoresis on a 15% acrylamide gel in TBE. Band intensities were quantified by densitometry, and the fraction unwound at each time point was determined from the ratio of substrate and product. Data were described by single-exponential functions to determine the rate constant k_{unwind}.

Steady-state ATPase activity

The ATPase activity of eIF4A was determined in a coupled enzymatic assay which couples ATP hydrolysis to NADH oxidation (28,60). Concentrations were 1 μM eIF4A, 2 μM eIF4E, 2 μM eIF4G, 2 μM eIF4B, 2 mM ATP, 0.4 mM NADH, 1 mM phosphoenolpyruvate, 23 μg/ml pyruvate kinase, 13 μg/ml lactate dehydrogenase, and 0 to 200 mM (bases of) RNA. Reactions were performed in 50 mM Tris/HCl pH 7.5, 80 mM KCl, 2.5 mM $MgCl_2$, 1 mM DTT and 1% (v/v) glycerol at 30°C in a transparent PS F-boden 384 well plate (Greiner bio-one) in a TECAN M1000 pro microplate reader. Reaction velocities were determined from the slopes of the absorbance curves. The dependence of the reaction velocities on the RNA concentration was described with the Michaelis-Menten equation to determine the k_{cat} for ATP hydrolysis and $K_{1/2}$ values for RNA.

Fluorescence labeling and single-molecule FRET experiments

Bio-eIF4A carrying cysteines in RecA_N (Q186C) and RecA_C (G370C) was labeled with a 2-fold molar excess of Alexa555-maleimide (A555, donor) and a 5-fold molar excess of Alexa647-maleimide (A647, acceptor). The labeling efficiency was determined from the absorption at 280, 554 and 647 nm.

For single-molecule FRET experiments, 5× activity buffer (250 mM Tris/HCl pH 7.5, 400 mM KCl, 12.5 mM $MgCl_2$, 5 mM DTT and 5% (v/v) glycerol) was treated with active charcoal overnight and filtered through a 0.4 μM membrane. All experiments were performed in activity buffer.

Experiments were performed with 150 pM labeled bio-eIF4A (donor concentration) in a BSA-saturated microwell slide (A10657-01, Hamamatsu) on a Picoquant Microtime 200 confocal microscope in the presence and absence of 8 μM eIF4G-A, 8–10 μM eIF4G-RA, 8 μM eIF4G-R*A, or 6 μM eIF4G-ERA, 6 μM eIF4E, 10 μM 50mer RNA (molar concentration) or 1 mM poly-U-RNA (concentration in bases), and 3 mM ATP at 25°C. Fluorescence intensities were corrected for donor crosstalk in the acceptor channel, acceptor crosstalk in the donor channel, different quantum yields and detection efficiencies of donor and acceptor fluorescence and direct excitation of the acceptor as previously described (61).

RESULTS

We previously showed that RNA3 of yeast eIF4G contributes to the stimulation of the conformational cycle of eIF4A and its ATPase and helicase activities (17,18). Here, we used a set of eIF4G deletion variants (Figure 1A) to further investigate the role of eIF4G domains in eIF4A activation: eIF4G-ERA comprises the 4E-BD, two of the three RNA binding domains (RNA2 and RNA3) and the eIF4A binding domain (4A-BD), and interacts with eIF4E and eIF4A (Supplementary Figure S1A,B). A shorter variant, eIF4G-RA, comprises RNA2, the 4A-BD and RNA3, but lacks the 4E-BD. This variant interacts with eIF4A, but not with eIF4E (Supplementary

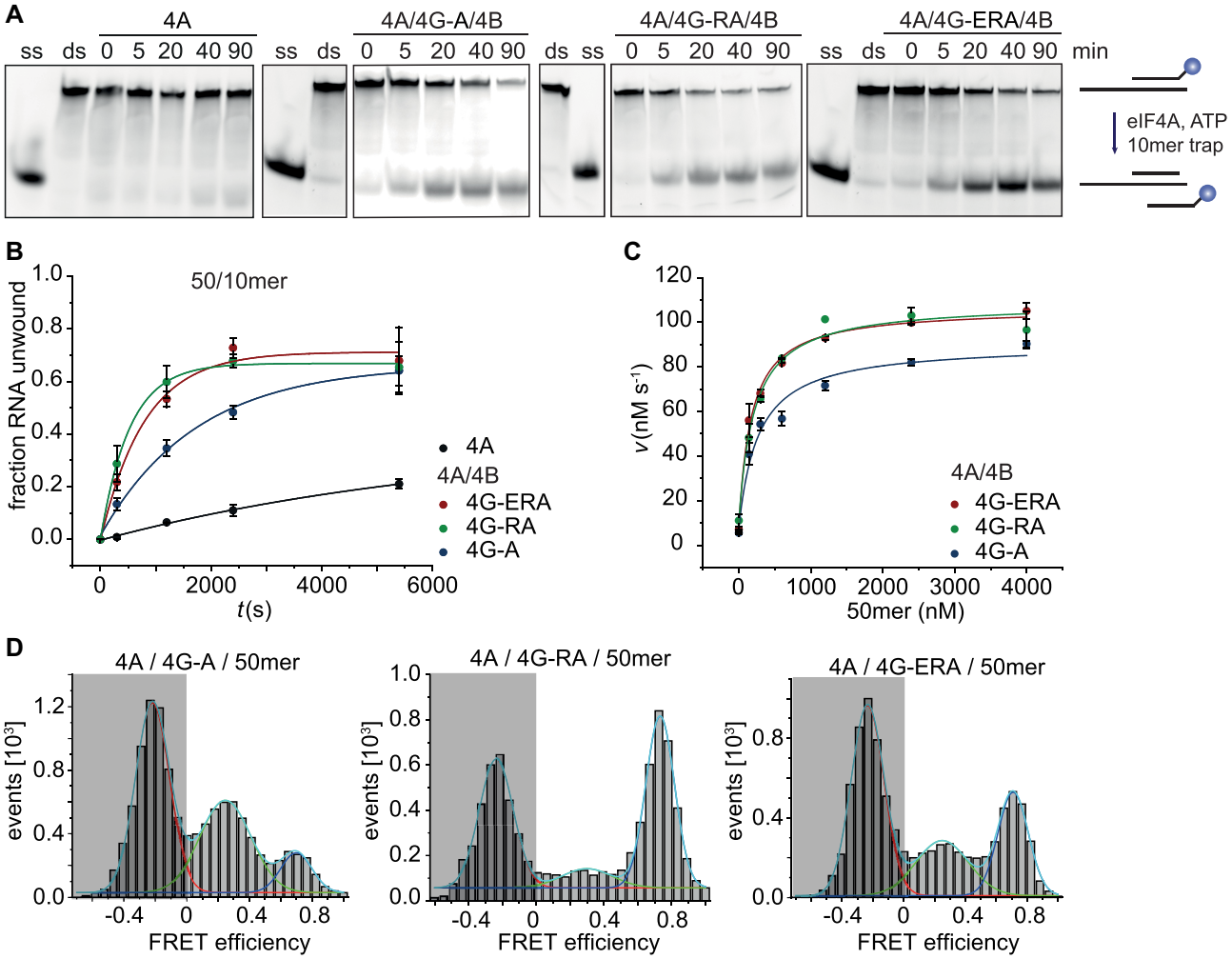

Figure 2. Effect of RNA2 on RNA unwinding, ATP hydrolysis and eIF4A conformation. (**A**) Representative unwinding reactions of 0.5 μM 50/10mer by eIF4A (5 μM) in the presence of 5 μM eIF4B and 5 μM eIF4G-A, eIF4G-RA or 4G-ERA in 50 mM Tris/HCl pH 7.5, 80 mM KCl, 2.5 mM $MgCl_2$, 1 mM DTT and 1% (v/v) glycerol. ss: single-stranded 10mer RNA, ds: double-stranded 50/10mer RNA. On the right-hand side, a schematic of the unwinding assay is shown; the blue sphere indicates the fluorescein attached to the 5′-end of the 10mer for fluorescence detection. Unwinding experiments were performed at least twice and gave similar results (see Supplementary Figure S3C). (**B**) Fraction of RNA unwound as a function of time, determined from densitometric quantification of single- and double-stranded RNA, for eIF4A (gray), eIF4A and eIF4G-A (blue), eIF4A and eIF4G-RA (green) or eIF4A and eIF4G-ERA (red). Error bars reflect the SEM from duplicate experiments. Rate constants for unwinding and reaction amplitudes are summarized in Table 1. See Supplementary Figure S2 for controls in the absence of ATP. (**C**) ATPase activity of 1 μM eIF4A in the presence of 50mer RNA (concentrations as indicated), 2 μM eIF4B and 2 μM eIF4G-ERA (red), eIF4G-RA (green) or eIF4G-A (blue) in 50 mM Tris/HCl pH 7.5, 80 mM KCl, 2.5 mM $MgCl_2$, 1 mM DTT, and 1% (v/v) glycerol. Error bars reflect the SEM from duplicate experiments. (**D**) Single-molecule FRET histograms of eIF4A in the presence of 50mer RNA and eIF4G-ERA, eIF4G-RA or eIF4G-A. In the presence of eIF4G-A, 25 ± 4% of eIF4A molecules are in the closed conformation, 76 ± 8% in the presence of eIF4G-RA and 61 ± 8% in the presence of eIF4G-ERA. Errors are the SEM from duplicate experiments. See Table 3 for a summary of the fraction closed. Green: half-open conformation of eIF4A with a FRET efficiency of 0.25, blue: closed conformation with a FRET efficiency of 0.70. FRET efficiencies below zero (red, marked by gray rectangles) result from donor-only labeled species. The cyan curve represents a fit of the sum of three Gaussian distributions to the data. Histograms show representative data; experiments were performed at least twice and gave similar results (see Supplementary Figure S6).

Figure S1B,C). Finally, eIF4G-A comprises the 4A-BD and RNA3, but lacks the 4E-BD and RNA2. This variant was termed eIF4G-MC in previous studies (16–18,51). As eIF4G-RA, eIF4G-A interacts with eIF4A, but not with eIF4E (Supplementary Figure S1A).

RNA2 plays a role in promoting eIF4A closing, its interaction with RNA, and RNA unwinding

To delineate the effect of RNA2 on RNA unwinding, we compared RNA unwinding activities of eIF4A in the presence of eIF4G-RA and 4G-A (Figure 2A, B), using a 50/10mer substrate employed previously to characterize eIF4A activities (16,17,51,62). This RNA substrate contains an unstructured 5′-single-stranded tail that mimics an unstructured 5′-UTR (Figure 1B). Reactions in the absence of ATP were performed as a negative control (Supplementary Figure S2). The low intrinsic helicase activity of eIF4A, with a rate constant of unwinding of k_{unwind} = 0.15 (± 0.03) × 10^{-3} s^{-1}, is stimulated both by eIF4G-A and eIF4G-RA (Figure 2A, B, Table 1). Consistent with previous observations (11,17,18), eIF4G-A

Table 1. Rate constants and amplitudes of unwinding reactions

		+ eIF4G-ERA		+ eIF4G-RA		+ eIF4G-A		– eIF4G	
		k_{unwind} (10^{-3} s^{-1})	ampl. (%)	k_{unwind} (10^{-3} s^{-1})	ampl. (%)	k_{unwind} (10^{-3} s^{-1})	ampl. (%)	k_{unwind} (10^{-3} s^{-1})	ampl. (%)
uncapped	- 4E	1.3 ± 0.2	72 ± 10	1.9 ± 0.2	67 ± 4	0.6 ± 0.1	66 ± 6	0.15 ± 0.03	n.d.
	+ 4E	0.53 ± 0.06	74 ± 1	1.4 ± 0.4	78 ± 6	0.5 ± 0.2	69 ± 6		
capped	- 4E	1.3 ± 0.1	79 ± 15	1.7 ± 0.2	93 ± 2	0.58 ± 0.07	61 ± 13	0.11 ± 0.0004	n.d.
	+ 4E	0.9 ± 0.3	84 ± 11	1.31 ± 0.07	90 ± 3	0.7 ± 0.1	75 ± 8		

Errors denote SD from triplicate experiments for 4A/4G-ERA/4E + capped RNA and for 4A/4G-A/4E + capped RNA. In all other cases, SEM from duplicate experiments are given; n.d.: not determined.

binding increases the rate constant of unwinding by eIF4A about 4-fold, to $k_{unwind} = 0.6 (\pm 0.1) \times 10^{-3}$ s^{-1}. In the presence of eIF4G-RA, unwinding is stimulated by 13-fold, with $k_{unwind} = 1.9 (\pm 0.2) \times 10^{-3}$ s^{-1} (Figure 2A, B, Table 1, Supplementary Figure S3A). These values correspond to a 3-fold stimulation of unwinding by RNA2. It is important to note that the stimulation factors contain contributions from stimulatory effects caused by the eIF4G variant present and by eIF4B. If eIF4B and 4G act cooperatively in stimulating RNA unwinding by eIF4A, with different levels of cooperativity for eIF4G-A and RA, these values constitute upper limits. The unwinding amplitudes are similar (~70%) with both eIF4G variants (Figure 2B, Supplementary Figure S3B).

The presence of RNA2 also had an effect on the ATPase activity of eIF4A (Figure 2C): In the presence of eIF4G-A, eIF4A hydrolyzed ATP with a turnover number of $k_{cat} = 83 (\pm 1) \times 10^{-3}$ s^{-1}. The stimulation of the ATPase activity by RNA is governed by a $K_{1/2} = 270 \pm 15$ nM. Both values are in agreement with previous reports (17,18). In the presence of eIF4G-RA containing RNA2, the turnover number was increased slightly, to $k_{cat} = 97 (\pm 3) \times 10^{-3}$ s^{-1}, at the same time $K_{1/2}$ for RNA was slightly decreased to $K_{1/2} = 212 \pm 20$ nM (Table 2A). Thus, RNA2 enhances the functional interaction of eIF4A with RNA.

We have shown previously that eIF4B also promotes functional RNA interactions with eIF4A, manifested as an approx. three-fold reduction on the $K_{1/2}$ value of eIF4A for RNA in the presence of eIF4B (16,18). We therefore tested whether the stimulatory effect of RNA2 is also present in the absence of eIF4B (Supplementary Figure S4A, B, Table 2B). Notably, the moderate effect of RNA2 observed in the presence of eIF4B becomes more pronounced when eIF4B is absent, with a three-fold decrease in $K_{1/2}$ (Table 2B).

eIF4A switches between different conformational states during ATP hydrolysis and RNA unwinding, which can be distinguished by their different FRET efficiencies in single-molecule FRET experiments (18,28). To test whether RNA2 has an effect on eIF4A conformation, we performed single-molecule FRET experiments with donor-acceptor-labeled eIF4A in the presence of eIF4G-A and eIF4G-RA (Figure 2D). In the presence of 50mer and ATP, we detected two different FRET states of eIF4A bound to eIF4G-A or eIF4G-RA: one with a FRET efficiency E_{FRET} of approx. 0.25, corresponding to the half-open state observed previously (28), and a second with E_{FRET} of approx. 0.70, corresponding to the closed state (18) (Figure 2D). These observations demonstrate that eIF4G-RA also stabilizes eIF4A in a half-open state, similar to eIF4G-A, and promotes eIF4A closing in the presence of ATP and RNA. The relative populations of the two states of eIF4A in the presence of eIF4G-A and eIF4G-RA differ, though: With eIF4G-A, 25 ± 4% of the eIF4A molecules are in the closed state. With eIF4G-RA this fraction is increased approx. three-fold, to 76 ± 8% (Figure 2D, Table 3), showing that the presence of RNA2 is associated with the promotion of the conformational change of eIF4A to the closed state. To test whether the increased capacity of eIF4G-RA to stimulate closing of eIF4A is caused by the interaction of RNA2 with RNA, we purified eIF4G-R*A, a construct comprising RNA2, the 4A-BD, and RNA3, in which twelve arginines within RNA2 are exchanged to alanines. These mutations had been reported to abrogate RNA binding to RNA2 (48). Anisotropy titrations demonstrate that mutation of these arginines has a similar deleterious effect on RNA binding as deletion of RNA2 (Supplementary Figure S5A). Single-molecule experiments with donor/acceptor-labeled eIF4A in the presence of eIF4G-R*A, poly-U-RNA, and ATP showed a significantly reduced fraction of eIF4A in the closed state compared to experiments in the presence of eIF4G-RA, similar to the observations with eIF4G-A lacking RNA2 (Supplementary Figure S5B). Altogether, the stimulatory effect of RNA2 on closing of eIF4A, its functional interaction with RNA, and its unwinding activity is thus linked to RNA binding to RNA2.

The 4E-BD partially reverts the stimulatory effects of RNA2

We next tested the effect of the 4E-BD of eIF4G on eIF4A activities, first in the absence of eIF4E (Figure 2). In the presence of eIF4G-ERA, eIF4A unwound the 50/10mer with a rate constant of $k_{unwind} = 1.3 (\pm 0.2) \times 10^{-3}$ s^{-1} (Figure 2A, Table 1). This value corresponds to a stimulation of its intrinsic unwinding activity by 9-fold, which is less than the stimulation achieved with eIF4G-RA (13-fold). Similarly, the fraction of eIF4A in the closed conformation was increased by eIF4G-ERA (fraction closed = 61 ± 8%; Figure 2D, Table 3), but less than with eIF4G-RA (76 ± 8%). Thus, the 4E-BD reduces the favorable effect of RNA2 on unwinding and closing of eIF4A. In contrast, the $K_{1/2}$ value of eIF4A for RNA, $K_{1/2} = 173 \pm 30$ nM, was slightly lower in the presence of

Table 2A. $K_{1/2}$ and k_{cat} values for RNA-dependent ATP hydrolysis by eIF4A in the presence of eIF4B and different eIF4G variants, and effects of eIF4E and the 5′-cap

		+ eIF4G-ERA		+ eIF4G-RA		+ eIF4G-A	
		$K_{1/2}$ (nM)	k_{cat} (10^{-3} s^{-1})	$K_{1/2}$ (nM)	k_{cat} (10^{-3} s^{-1})	$K_{1/2}$ (nM)	k_{cat} (10^{-3} s^{-1})
uncapped	− 4E	173 ± 30	99 ± 1	212 ± 20	97 ± 3	270 ± 15	83 ± 1
	+ 4E	199 ± 28	100 ± 3	193 ± 39	92 ± 14	457 ± 38	82 ± 1
capped	− 4E	304 ± 6	81 ± 1	342 ± 31	92 ± 4	553 ± 193	89 ± 9
	+ 4E	294 ± 41	74 ± 4	374 ± 56	88 ± 6	975 ± 27	89 ± 3

Errors are SEM from duplicate experiments.

Table 2B. $K_{1/2}$ and k_{cat} values for RNA-dependent ATP hydrolysis by eIF4A in the presence of different eIF4G variants, and effects of eIF4E and the 5′-cap (no eIF4B present)

		+ eIF4G-ERA		+ eIF4G-RA		+ eIF4G-A	
		$K_{1/2}$ (nM)	k_{cat} (10^{-3} s^{-1})	$K_{1/2}$ (nM)	k_{cat} (10^{-3} s^{-1})	$K_{1/2}$ (nM)	k_{cat} (10^{-3} s^{-1})
uncapped	− 4E	290 ± 28	94 ± 8	355 ± 0	100 ± 2	1053 ± 139	80 ± 9
	+ 4E	343 ± 57	96 ± 5	240 ± 30	84 ± 5	1864 ± 286	88 ± 1
capped	− 4E	533 ± 13	88 ± 9	444 ± 23	112 ± 8	1611 ± 178	78 ± 4
	+ 4E	650 ± 95	93 ± 6	525 ± 53	95 ± 5	2767 ± 1537	90 ± 34

Errors are SEM from duplicate experiments.

Table 3. Fraction of eIF4A in the closed state in the presence of different eIF4G variants, and effects of eIF4E and the 5′-cap

		fraction closed (%)		
		+ eIF4G-ERA	+ eIF4G-RA	+ eIF4G-A
uncapped	− 4E	61 ± 8	76 ± 8	25 ± 4
	+ 4E	49 ± 4	80 ± 3	27 ± 7
capped	− 4E	56 ± 0.5	76 ± 3	12 ± 4
	+ 4E	52 ± 3	66 ± 1	20 ± 3

Errors are SEM from duplicate experiments.

eIF4G-ERA compared to eIF4G-RA ($K_{1/2} = 212 \pm 20$ nM; Figure 2C, Table 2A), in agreement with an additional, positive effect of the 4E-BD on the interaction of eIF4A with RNA. This effect was also observed in the absence of eIF4B (Table 2B). The k_{cat} values were similar in the absence and presence of the 4E-BD (Table 2A, 2B).

Notably, eIF4A/4G-ERA also unwound RNA in the absence of ATP (Supplementary Figure S2A, B). This reaction occurred on a comparable timescale to ATP-dependent unwinding, and reached a similar reaction amplitude. Such an effect was not observed with eIF4A and eIF4G-A or 4G-RA. As the protocols for purification of eIF4G-ERA and -RA are very similar, we consider it unlikely that the ATP-independent duplex destabilization in the presence of 4G-ERA is caused by a contaminating helicase. Instead, we suspect that it may related to (single-stranded) RNA binding by 4G-ERA. The absence of this background activity in the presence of 4G-RA suggests that this effect may require the presence of both RNA2 and the 4E-BD.

Altogether, the 4E-BD shows effects antagonistic to RNA2 on eIF4A unwinding and closing, but both domains promote the functional interaction of eIF4A with RNA.

eIF4E reduces the unwinding activity of eIF4A/4G and the fraction of eIF4A in the closed state, but does not alter the ATPase activity and the functional interaction with RNA

We next tested how eIF4E affects eIF4A/4G activities (Figure 3). First, we investigated the effect of eIF4F formation by adding eIF4E to eIF4A in the presence of 4G-ERA, which contains the 4E-BD and interacts with eIF4E (Supplementary Figure S1A, B). The eIF4A/4G-ERA/4E complex showed a 2- to 3-fold reduced k_{unwind} compared to eIF4A/4G-ERA, with $k_{unwind} = 1.3\ (\pm 0.2) \times 10^{-3}$ s^{-1} in the absence and $k_{unwind} = 0.53\ (\pm 0.06) \times 10^{-3}$ s^{-1} in the presence of eIF4E (Figure 3A,B, Table 1). Such a reduction in the rate constant of unwinding was not observed in the absence of the 4E-BD, on the addition of eIF4E to eIF4A/4G-RA or eIF4A/4G-A (Figure 3A,B, Table 1). Hence, the observed inhibitory effect of eIF4E on unwinding by eIF4A/4G-ERA requires the 4E-BD and is the result of eIF4F formation. The amplitudes of the unwinding reactions for eIF4A/4G and eIF4F are similar, with 70% RNA unwound after 90 min (Figure 3B, Supplementary Figure S3B). In the presence of eIF4E, ATP-independent duplex destabilization by eIF4A/4G-ERA was suppressed to background levels, similar to the unspecific unwinding observed with eIF4A alone (Supplementary Figure S2A, B), indicating that binding of eIF4E to the 4E-BD alters the interaction of the 4E-BD and RNA2 with RNA.

We also tested the effect of eIF4E on the ATPase activity of eIF4A (Figure 3C, Table 2A, B). eIF4E did not affect the k_{cat} or $K_{1/2}$ value of eIF4A/4G-ERA for RNA. Thus, the functional interaction of eIF4F (comprising eIF4G-ERA) and eIF4A/4G with RNA is similar. As a control for unspecific effects of eIF4E, we also tested if eIF4E altered the ATPase activity of eIF4A/4G-A and eIF4A/4G-RA (Figure 3C, Table 2A, B). eIF4E had little effect on the

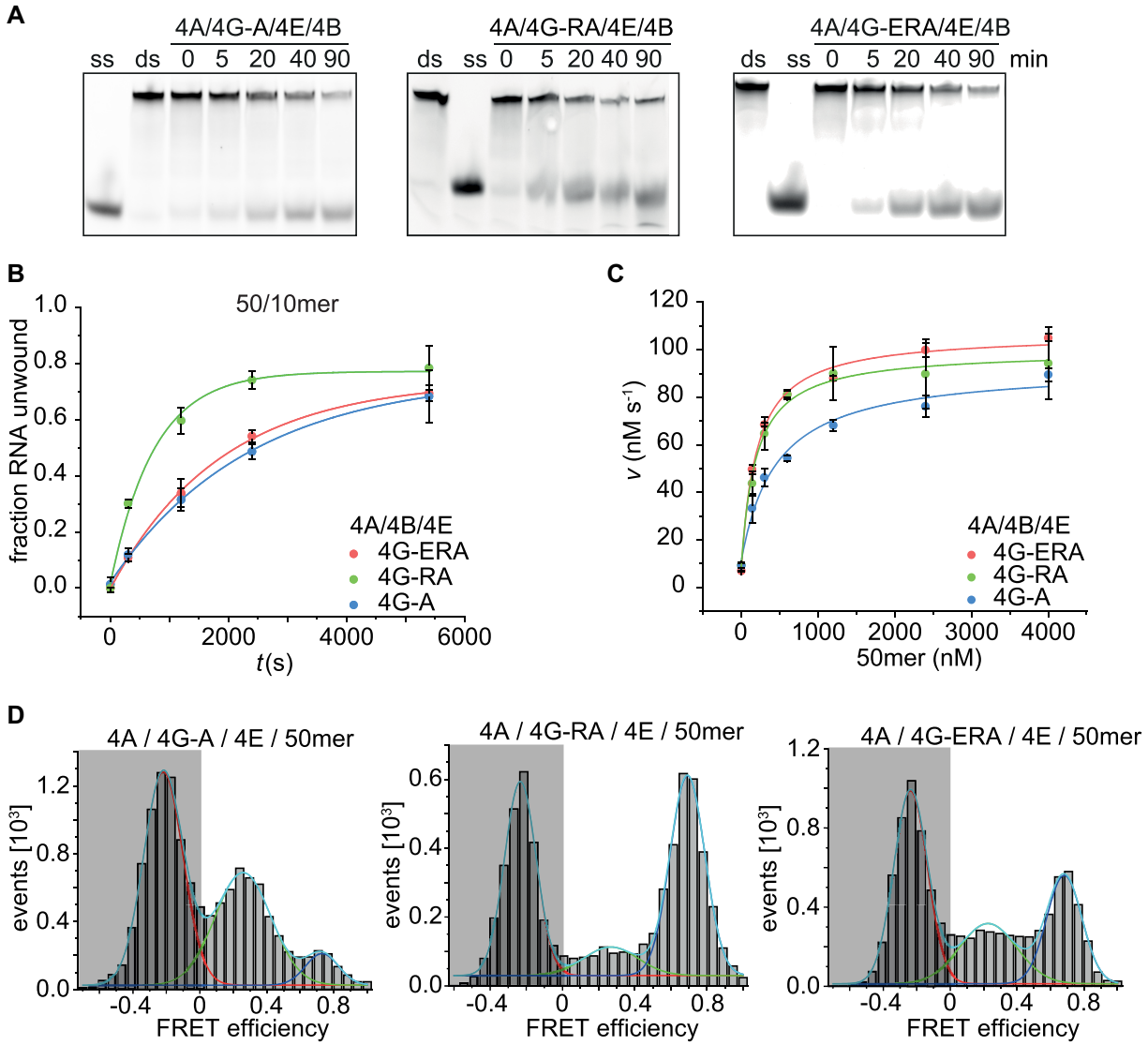

Figure 3. Effect of eIF4E on RNA unwinding, ATPase activity and eIF4A conformation. (**A**) Representative unwinding reactions of 0.5 μM 50/10mer RNA by 1 μM eIF4A in the presence of 5 μM eIF4E, 5 μM eIF4B and 5 μM eIF4G-A, eIF4G-RA or eIF4G-ERA, analysed by native polyacrylamide gel electrophoresis. For reaction conditions, see legend to Figure 2A. (**B**) Fraction of RNA unwound as a function of time, determined from densitometric quantification of single- and double-stranded RNA, for eIF4A, eIF4B, eIF4E and eIF4G-ERA (red), eIF4G-RA (green) or eIF4G-A (blue). Error bars depict the SEM from duplicate experiments. Rate constants of unwinding and amplitudes are summarized in Table 1 (see Supplementary Figure S3B). (**C**) ATPase activity of 1 μM eIF4A in the presence of 50mer RNA (concentrations indicated), 2 μM eIF4B, 2 μM eIF4E and 2 μM eIF4G-ERA (red), eIF4G-RA (green) or eIF4G-A (blue). For reaction conditions, see legend to Figure 2C. Error bars depict the SEM from duplicate experiments. (**D**) Single-molecule FRET histograms of eIF4A in the presence of eIF4E, 50mer RNA and eIF4G-ERA, eIF4G-RA or eIF4G-A. In the presence of eIF4G-A and eIF4E, 27 ± 7% of eIF4A molecules adopt the closed conformation, 80 ± 3% in the presence of eIF4G-RA, and 49 ± 4% in the presence of eIF4G-ERA. Errors are the SEM from duplicate experiments. Histograms show representative data; experiments were performed at least twice with similar results (see Supplementary Figure S6). See Table 3 for a summary of the fraction closed. Green: half-open conformation of eIF4A with a FRET efficiency of 0.25, blue: closed conformation with a FRET efficiency of 0.70. FRET efficiencies below zero (red, marked by gray rectangles) result from donor-only labeled species. The cyan curve represents a fit of the sum of three Gaussian distributions to the data.

k_{cat} values, but led to a slight, almost 2-fold increase in the $K_{1/2}$ value of eIF4A/4G-A for RNA (Figure 3C, Table 2A, B), but not for eIF4G-RA. eIF4E does not interact with eIF4G-A (Supplementary Figure S1B, C), suggesting that this inhibitory effect must be indirect, possibly mediated through (cap-independent) interactions of eIF4E with the RNA. Apparently, this indirect effect is overcompensated by the positive effect of RNA2 on RNA binding in eIF4G-RA and eIF4G-ERA.

We next performed single-molecule FRET experiments to test the effect of eIF4E on eIF4A conformation (Figure 3D). Again, we first analyzed the effect on eIF4F formation, i.e. in the presence of the 4E-BD. Addition of eIF4E to the eIF4A/4G-ERA complex was accompanied by a decrease in the fraction closed, from 61 ± 8% with eIF4A/4G-ERA to 49 ± 4% when eIF4E was bound (Figure 3D, Table 3). In the absence of the 4E-BD, i.e. with eIF4A/4G-A and with eIF4A/4G-RA, the fraction of eIF4A in the closed

state did not change on eIF4E addition, and remained at 27 ± 7% with eIF4A/4G-A (versus 25 ± 4% in the absence of 4E) and 80 ± 3% with eIF4A/G-RA (versus 76 ± 8% in the absence of 4E, Figure 3D, Table 3). Thus, the decrease in the fraction of eIF4A in the closed state when eIF4G-ERA is present requires the presence of the 4E-BD, and is a consequence of eIF4F formation. As observed in the absence of eIF4E, eIF4G-RA also has a more pronounced stimulatory effect on eIF4A closing than eIF4G-ERA in the eIF4F complex.

In summary, eIF4E binding to the 4E-BD thus decreases the helicase activity of eIF4A and reduces the fraction of eIF4A in the closed state, but does not affect the interaction with RNA.

The 5′-cap does not affect RNA unwinding and eIF4A closing, but leads to less efficient binding of RNA to eIF4A

In the next set of experiments, we investigated the role of the 5′-cap on eIF4A activities and conformation. Overall, capped RNA was unwound with similar rate constants as uncapped RNA (Figure 4A, B, Supplementary Figure S3A, B, Table 1). Similar as with uncapped RNA, we observed a stimulatory effect of RNA2, manifested in a higher rate constant of unwinding in the presence of eIF4G-RA compared to 4G-A, and an inhibitory effect of the 4E-BD, evident from the reduced rate constant of unwinding with eIF4G-ERA compared to 4G-RA. The inhibitory effect of eIF4E on RNA unwinding was also observed, but it was less pronounced with capped than with uncapped RNA (Figure 4B, Table 1).

Although the presence of the cap had no global effect on RNA unwinding, we observed a tendency for capped RNA to be unwound slightly faster than uncapped RNA in the presence of the 4E-BD and eIF4E (Figure 4B, Table 1), i.e. for eIF4A/4G-ERA/4E (Table 1), in agreement with a minor stimulatory effect of the cap/4E interaction on RNA unwinding. Consistent with this notion, unwinding of capped and uncapped RNAs occurred with virtually identical velocities in the presence of 4G-A and 4G-RA, which lack the 4E-BD and cannot interact with eIF4E (Figure 4A,B, Supplementary Figure S3A).

We then determined the effect of the 5′-cap on ATP hydrolysis by eIF4A (Figure 4C, Table 2A). The 5′-cap itself had no effect on the k_{cat} values, but the presence of the 5′-cap was consistently associated with higher $K_{1/2}$ values for the RNA (Figure 4C, Table 2A), independent of the presence of eIF4E or the nature of the 4G variant present. This increase in $K_{1/2}$ was also independent of eIF4B (Table 2A, B). As observed with uncapped RNA, the $K_{1/2}$ value for RNA was lower with 4G-ERA and 4G-RA than with eIF4G-A, in agreement with a higher RNA affinity of eIF4A/4G when RNA2 is present (Figure 4C, Table 2A, B). In contrast, the 4E-BD did not show the antagonistic effect to RNA2 on $K_{1/2}$ when the 5′-cap was present, manifested in similar values in the presence of eIF4G-ERA and eIF4G-RA. With capped RNA, eIF4E also had no effect on k_{cat} or $K_{1/2}$ values of eIF4A in the presence of the 4E-BD. eIF4E led to the same slight, less than two-fold increase in the $K_{1/2}$ value of eIF4A/4G-A in the presence of the cap, indicating that its unspecific, indirect effect on eIF4A is cap-independent.

Finally, we tested the effect of the 5′-cap on eIF4A conformation. (Figure 4D, Supplementary Figure S6A). Overall, the cap either had no effect or led to a slight reduction of the fraction closed. As in the absence of the cap, the fraction closed was lowest in the presence of eIF4G-A, and highest in the presence of eIF4G-RA (Figure 4D), consistent with a stimulatory effect of RNA2 and an inhibitory effect of the 4E-BD on closing. Again, this effect was observed both in the presence and in the absence of eIF4E (Figure 4D, Supplementary Figure S6B). As observed with uncapped RNA, eIF4E thus shows no consistent effect on eIF4A conformation. The most prominent effect observed in the presence of the cap is an increased stimulatory effect of eIF4G-RA and -ERA on eIF4A closing (from 2–3-fold compared to 4G-A to 5–6-fold), which is restored to the level observed with uncapped RNA (2–3-fold) when eIF4E is also present.

The stimulation of the eIF4A ATPase activity by eIF4B is independent of the eIF4E/4G interaction and the 5′-cap

In previous studies we reported a stimulatory effect of eIF4B on ATP hydrolysis by eIF4A in the presence of eIF4G-A, manifested as a decrease in $K_{1/2}$ when eIF4B is present (18). Above, we showed that RNA2 of eIF4G also leads to a decrease in $K_{1/2}$ of eIF4A for RNA. This effect is pronounced in the absence of eIF4B, but smaller when eIF4B is present, indicating that both RNA2 and eIF4B stimulate the interaction of eIF4A with RNA through the same mechanism. Here, we asked whether the effect of eIF4B depends on eIF4E and the 5′-cap. Notably, the $K_{1/2}$ values are reduced on addition of eIF4B irrespective of the eIF4G variant present, independent of the presence of eIF4E, and independent of the presence of the 5′-cap (Figure 5A). In contrast, k_{cat} values are not affected much by eIF4B addition (Figure 5B), as observed previously (18). For all eIF4G variants, the lowest $K_{1/2}$ values for RNA are observed in the presence of eIF4B and uncapped RNA, whereas $K_{1/2}$ values are highest in the presence of eIF4E and the 5′-cap. The presence of eIF4B thus leads to a global increase in the apparent RNA affinity of eIF4A, both for capped and uncapped RNA.

DISCUSSION

In this work, we investigated the interplay of eIF4G and its domains, of eIF4E, and of the 5′-cap in regulating conformational cycling as well as ATPase and helicase activities of yeast eIF4A. In humans, an autoinhibitory effect of the 4E-BD of eIF4G on the capacity of eIF4G to stimulate the eIF4A helicase activity has been reported (13); this effect is alleviated on binding of eIF4E to the 4E-BD. We show here that, in contrast to these observations, the 4E-BD does not interfere with eIF4A activation in yeast, pointing to different regulatory mechanisms in translation initiation in yeast and humans. From the different domain structures, particularly of eIF4G and eIF4B, in both organisms, more differences in the functional interplay of translation initiation factors in yeast and humans can be expected.

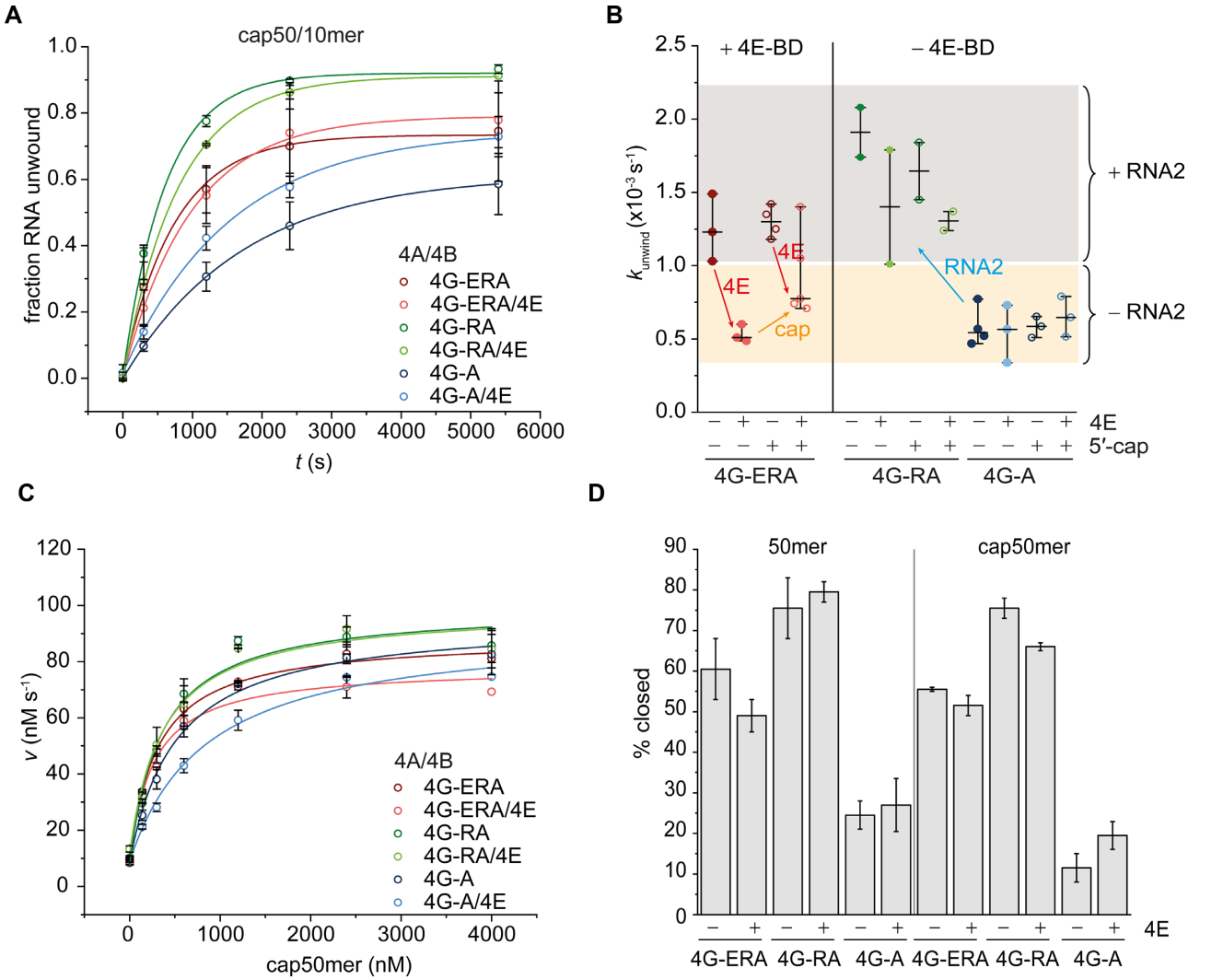

Figure 4. Effect of the 5′-cap on RNA unwinding, ATPase activity and eIF4A conformation. (**A**) Effect of eIF4E on unwinding of the capped 50/10mer by eIF4A in the presence of eIF4B and eIF4G-ERA (red), eIF4G-RA (green) or eIF4G-A (blue). For reaction conditions, see legend to Figure 2A. Error bars depict the SD from triplicate experiments for 4A/4G-ERA/4E and for 4A/4G-A/4E. In all other cases, SEM from duplicate experiments are shown. Rate constants of unwinding and amplitudes are summarized in Table 1. (**B**) Rate constants of unwinding in the presence of different eIF4G variants in the presence and absence of eIF4E, and with uncapped and capped 50/10mer RNA. Horizontal lines indicate the mean value, errors bars the standard error of the mean from at least two independent experiments. See Figures 1, 2 and Supplementary Figure S3 for original data and quantifications.(**C**) Effect of eIF4E (2 μM) on the ATPase activity of eIF4A (1 μM) in the presence of capped 50mer RNA (concentrations as indicated), eIF4B (2 μM) and 2 μM eIF4G-ERA (red), eIF4G-RA (green) or eIF4G-A (blue) in 50 mM Tris/HCl pH 7.5, 80 mM KCl, 2.5 mM $MgCl_2$, 1 mM DTT and 1% (v/v) glycerol. Error bars depict the SEM from duplicate experiments. (**D**) Effect of eIF4E and the 5′-cap on the closed population of eIF4A in the presence of eIF4G-ERA, eIF4G-RA or eIF4G-A. For single-molecule FRET histograms see Figures 1 and 2 and Supplementary Figure S6. Error bars denote the standard error of the mean from two independent experiments.

Interplay of the eIF4G domains, eIF4B, eIF4E and the cap in the activation of eIF4A

Although our experimental system is limited to a subset of factors and does not recapitulate all aspects of translation initiation, it provides important insight into the functional interplay of eIF4E, 4G and 4B with eIF4A at the cap (Figure 6). We have previously shown that the presence of the C-terminal RNA-binding region, RNA3, in yeast eIF4G is associated with an increased stimulation of eIF4A conformational cycling, a stronger ATP-dependent interaction of eIF4A with RNA, and a moderate increase in the rate constant of unwinding (17,18). Here, we show that RNA2 also provides an RNA binding site that is functionally coupled to the ATPase and helicase activities of eIF4A. We posit that binding of RNA2 to the mRNA might alter the RNA conformation preceding the RNA duplex bound to eIF4A, which decreases the activation barrier for duplex destabilization and enables faster unwinding. The stimulatory effect of RNA2 on eIF4A unwinding activity is paralleled by an increase in the fraction of eIF4A in the closed conformation when RNA2 is present (Figure 6). This observation implies that, similar to RNA3, RNA2 also accelerates closing of eIF4A relative to opening. The stimulation of RNA unwinding by RNA2 and RNA3 is smaller than reported previously in the context of eIF4G,

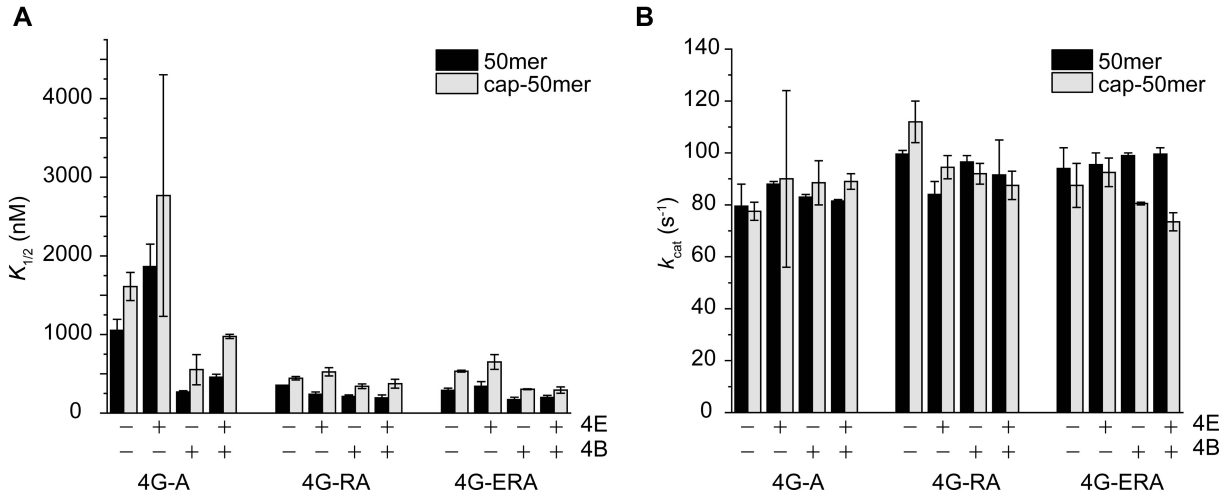

Figure 5. Effect of eIF4B on RNA unwinding and ATP hydrolysis. (**A**) Effect of eIF4B, eIF4E, eIF4G, and the 5′-cap on $K_{1/2}$ values for RNA. (**B**) Effect of eIF4B, eIF4E, eIF4G, and the 5′-cap on k_{cat} values. Errors are the SEM from two independent experiments. See Supplementary Figure S4 for original data in the absence of eIF4B.

additionally comprising the most N-terminal RNA-binding region RNA1 (14), suggesting that RNA1 may act as an amplifier of these effects. The prominent favorable effect of RNA2 on the ATPase stimulation by RNA observed in the absence of eIF4B is dwarfed when eIF4B is present. In turn, the favorable effect of eIF4B on stimulation of the eIF4A ATPase activity observed previously (16–18) is substantially reduced when RNA2 is present (see Table 2A, B). This coupling suggests that both RNA2 and eIF4B anchor eIF4A on the RNA through the same mechanism.

The 4E-BD of eIF4G partially counteracts the stimulatory effect of RNA2 on the helicase activity of eIF4A and on the fraction of eIF4A in the closed conformation. This antagonistic effect of the 4E-BD and RNA2 may be caused by an altered interaction of RNA2 with the RNA when the adjacent 4E-BD is present. In contrast to its effect on unwinding, the 4E-BD does not counteract the favorable effect of RNA2 on the functional interaction of the RNA with eIF4A, but instead leads to a slight additional increase in RNA affinity (Figure 6). These differential effects indicate that the inhibitory effect of the 4E-BD is not a mere reversal of the stimulatory effect of RNA2, but must be mechanistically distinct. The enhancing effect of the 4E-BD on RNA binding is independent of the presence of eIF4B, implying that the 4E-BD and eIF4B employ different modes of action to strengthen the interaction of eIF4A with RNA.

Binding of eIF4E to the 4E-BD upstream of RNA2 then completely resets the rate constant of unwinding to the value observed in the absence of RNA2. The inhibitory effect of eIF4E is dependent on the presence of the 4E-BD, and thus on the 4E-BD/4E interaction. In contrast to its inhibitory effect on RNA unwinding, eIF4E engaged to the 4E-BD does not alter the interaction of eIF4A with RNA or the conformational equilibrium of eIF4A (Figure 6). This disparate behavior further supports different modes of action of RNA2 on one hand and the 4E-BD and 4E on the other hand.

Finally, the presence of the cap has little effect on unwinding, in agreement with previous observations (14), or on the eIF4A conformational equilibrium. Instead, it leads to a decrease in RNA affinity. This effect is independent of the presence of RNA2 in eIF4G and of eIF4B, supporting the notion that the cap on one hand and RNA2 and eIF4B on the other hand use different mechanisms to modulate the interaction of eIF4A with RNA. Altogether, our results demonstrate that the fine-tuning of eIF4A activities within the eIF4F complex is achieved through an intricate interplay between individual domains of eIF4G, eIF4A, eIF4E, the mRNA and its 5′-cap.

The 5′-cap/4E interaction plays a minor role for eIF4F assembly on the mRNA

The reduction of the RNA affinity of eIF4A in presence of the 5′-cap is a global effect, independent of the presence of eIF4E and the eIF4E/cap interaction. The inhibitory effect of eIF4E on RNA unwinding by eIF4A, depends on the presence of the 4E-BD, but is also independent of the presence of the cap, and thus of the 4E/5′-cap interaction. Finally, the eIF4E-induced increase in $K_{1/2}$ for RNA, observed even in the absence of the 4E-BD, also occurs independent of the cap and the 4E/cap interaction. Collectively, these observations are consistent with previous reports suggesting that the eIF4E/cap interaction is not important for the assembly of the eIF4F complex or for functional interactions between its components during cap recognition, but may become important for steps subsequent to eIF4F binding to the mRNA (29,63).

Different enzymatic properties of eIF4A, eIF4A/4G, and eIF4F: implications for eIF4F assembly and the mechanism of translation initiation

Here and in previous work (17,18,28) we have shown that yeast eIF4A, eIF4A/4G and eIF4F differ substantially

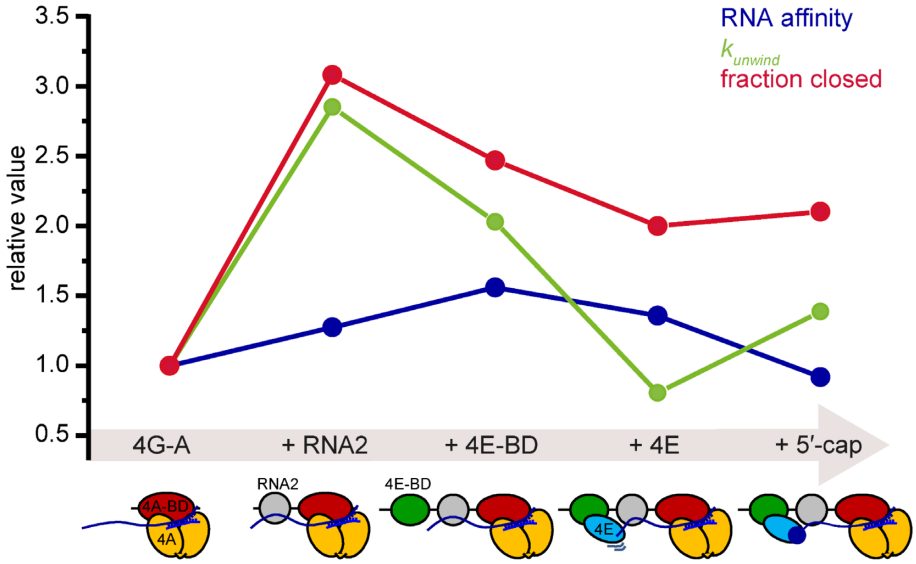

Figure 6. Summary of effects of RNA2, the 4E-BD, eIF4E and the cap on eIF4A. Changes in the rate constant of unwinding (green), the fraction of eIF4A in the closed conformation (red), and the RNA affinity (blue, inverse of $K_{1/2}$ values) of eIF4A. Values for eIF4G-A (4G-A) were set to one. The cartoons below depict the different eIF4s and the domains of eIF4G. Yellow: eIF4A, red: 4A-BD of eIF4G, gray: RNA2 of eIF4G, green: 4E-BD of eIF4G, light blue: eIF4E, dark blue circle: 5′-cap. The RNA is depicted in dark blue and blue.

in their enzymatic properties. Due to the large excess of eIF4A in yeast over eIF4G and, to a lesser extent, eIF4E (26), only 4% of eIF4A are present in the eIF4F complex under cellular conditions, which corresponds to 1–2 eIF4F complexes per mRNA on average (26), making eIF4F a limiting factor for translation initiation in yeast. The largest part, 96%, of eIF4A in the cell remains unbound (26). With its low basal activity (17,56,57), free eIF4A may not be able support cap recognition and PIC recruitment on structured mRNA 5′-ends. However, this free eIF4A could contribute to remodeling of downstream regions of the 5′-UTR or mRNA in multiple association-dissociation cycles, acting as a general RNA chaperone. Our results would thus support a model in which the eIF4F complex acts exclusively at the cap, whereas free eIF4A functions outside the cap in downstream processes (31).

eIF4A, 4G, and 4E assemble *de novo* at the 5′-cap for each round of translation (64). While it has classically been assumed that assembly is initiated by eIF4E binding to the 5′-cap (7,8), a recent single-molecule study suggested that binding of eIF4G to a 5′-single-stranded overhang of the mRNA might precede association of eIF4E with the cap (27,42). Such an early interaction of eIF4G with the mRNA could be relevant under physiological conditions, where eIF4G concentrations are limiting for eIF4F formation (26). eIF4G binding leads to a conformational change of the RNA (27) and may remove secondary structure elements near the cap. eIF4G binding would thus prepare the assembly intermediate for joining of eIF4E (27) and enable its rapid and stable association with the 5′-cap (27,40). The order of events during eIF4F assembly may be similar in humans, where binding of eIF4G to the mRNA also facilitates binding of eIF4E (41).

Our data provide a mechanistic framework for eIF4F assembly in yeast: According to eIF4 affinities and cellular concentrations (11,26,28), any eIF4G interacting with the 5′-UTR would be bound to eIF4A. We show here that this eIF4A/4G assembly intermediate constitutes an activated form of eIF4A, in which eIF4A spends more time in the closed state, its ATPase activity is efficiently stimulated by RNA, and RNA is rapidly unwound (this work and (17,28)). This complex is thus ideally suited to remove secondary structures at the cap with high efficiency to pave the way for eIF4E binding. The subsequent association of eIF4E with eIF4G and the 5′-cap structure then serves to anchor the resulting eIF4F complex at the 5′-end of the mRNA (27,40), completing eIF4F assembly. The intricate interplay between RNA2, the 4E-BD, 4E and the cap converts the yeast eIF4F complex into a slower helicase, although ATP hydrolysis is still stimulated efficiently by RNA. eIF4E binding thus acts as a brake for eIF4A unwinding activity, but enhances the anchoring of eIF4A on the RNA, which may support a continuous helicase activity during scanning.

It is currently unclear whether scanning of yeast mRNAs occurs in a cap-tethered fashion, with the eIF4G/4E interaction maintained until the start codon is reached. In general, it is not known at which stage during scanning individual eIF4 factors might dissociate from the PIC. Selective 40S subunit profiling as well as single-molecule studies of translation initiation (27,42,65–67) hold great potential in dissecting the assembly pathways of eIF4s along the initiation process, both for specific mRNAs and transcriptome-wide. Such studies will help pin-point the distinct roles of the individual eIF4 factors and their complexes in the different stages of translation initiation on different mRNAs.

DATA AVAILABILITY

Data are available from the authors on reasonable request.

SUPPLEMENTARY DATA

Supplementary Data are available at NAR Online.

ACKNOWLEDGEMENTS

We thank Jessica Guddorf and Daniela Schlingmeier for excellent technical assistance.

FUNDING

DFG [KL-1153/7-1, 7-2 to D.K.]. The open access publication charge for this paper has been waived by Oxford University Press - *NAR* Editorial Board members are entitled to one free paper per year in recognition of their work on behalf of the journal.
Conflict of interest statement. None declared.

REFERENCES

1. Shirokikh,N.E. and Preiss,T. (2018) Translation initiation by cap-dependent ribosome recruitment: recent insights and open questions. *Wiley Interdiscip. Rev. RNA*, **9**, e1473.
2. Marintchev,A. (2013) Roles of helicases in translation initiation: a mechanistic view. *Biochim. Biophys. Acta*, **1829**, 799–809.
3. Hinnebusch,A.G. and Lorsch,J.R. (2012) The mechanism of eukaryotic translation initiation: new insights and challenges. *Cold Spring Harb. Perspect. Biol.*, **4**, a011544.
4. Jackson,R.J., Hellen,C.U. and Pestova,T.V. (2010) The mechanism of eukaryotic translation initiation and principles of its regulation. *Nat. Rev. Mol. Cell Biol.*, **11**, 113–127.
5. Grifo,J.A., Tahara,S.M., Morgan,M.A., Shatkin,A.J. and Merrick,W.C. (1983) New initiation factor activity required for globin mRNA translation. *J. Biol. Chem.*, **258**, 5804–5810.
6. Neff,C.L. and Sachs,A.B. (1999) Eukaryotic translation initiation factors 4G and 4A from *Saccharomyces cerevisiae* interact physically and functionally. *Mol. Cell. Biol.*, **19**, 5557–5564.
7. Altmann,M., Handschin,C. and Trachsel,H. (1987) mRNA cap-binding protein: cloning of the gene encoding protein synthesis initiation factor eIF-4E from *saccharomycescerevisiae*. *Mol. Cell. Biol.*, **7**, 998–1003.
8. Sonenberg,N., Morgan,M.A., Merrick,W.C. and Shatkin,A.J. (1978) A polypeptide in eukaryotic initiation factors that crosslinks specifically to the 5′-terminal cap in mRNA. *Proc. Natl. Acad. Sci. U.S.A.*, **75**, 4843–4847.
9. Gross,J.D., Moerke,N.J., von der Haar,T., Lugovskoy,A.A., Sachs,A.B., McCarthy,J.E. and Wagner,G. (2003) Ribosome loading onto the mRNA cap is driven by conformational coupling between eIF4G and eIF4E. *Cell*, **115**, 739–750.
10. Gruner,S., Peter,D., Weber,R., Wohlbold,L., Chung,M.Y., Weichenrieder,O., Valkov,E., Igreja,C. and Izaurralde,E. (2016) The structures of eIF4E-eIF4G complexes reveal an extended interface to regulate translation initiation. *Mol. Cell*, **64**, 467–479.
11. Schutz,P., Bumann,M., Oberholzer,A.E., Bieniossek,C., Trachsel,H., Altmann,M. and Baumann,U. (2008) Crystal structure of the yeast eIF4A-eIF4G complex: an RNA-helicase controlled by protein-protein interactions. *Proc. Natl. Acad. Sci. U.S.A.*, **105**, 9564–9569.
12. Svitkin,Y.V., Pause,A., Haghighat,A., Pyronnet,S., Witherell,G., Belsham,G.J. and Sonenberg,N. (2001) The requirement for eukaryotic initiation factor 4A (elF4A) in translation is in direct proportion to the degree of mRNA 5′ secondary structure. *RNA*, **7**, 382–394.
13. Feoktistova,K., Tuvshintogs,E., Do,A. and Fraser,C.S. (2013) Human eIF4E promotes mRNA restructuring by stimulating eIF4A helicase activity. *Proc. Natl. Acad. Sci. U.S.A.*, **110**, 13339–13344.
14. Rajagopal,V., Park,E.H., Hinnebusch,A.G. and Lorsch,J.R. (2012) Specific domains in yeast eIF4G strongly bias the RNA unwinding activity of the eIF4F complex towards duplexes with 5′-overhangs. *J. Biol. Chem.*, **287**, 20301–20312.
15. Rogers,G.W., Richter,N.J. Jr, Lima,W.F. and Merrick,W.C. (2001) Modulation of the helicase activity of eIF4A by eIF4B, eIF4H, and eIF4F. *J. Biol. Chem.*, **276**, 30914–30922.
16. Andreou,A.Z., Harms,U. and Klostermeier,D. (2016) eIF4B stimulates eIF4A ATPase and unwinding activities by direct interaction through its 7-repeats region. *RNA Biol.*, **14**, 113–123.
17. Harms,U., Andreou,A.Z., Gubaev,A. and Klostermeier,D. (2014) eIF4B, eIF4G and RNA regulate eIF4A activity in translation initiation by modulating the eIF4A conformational cycle. *Nucleic Acids Res.*, **42**, 7911–7922.
18. Andreou,A.Z. and Klostermeier,D. (2014) eIF4B and eIF4G jointly stimulate eIF4A ATPase and unwinding activities by modulation of the eIF4A conformational cycle. *J. Mol. Biol.*, **426**, 51–61.
19. Sun,Y., Atas,E., Lindqvist,L., Sonenberg,N., Pelletier,J. and Meller,A. (2012) The eukaryotic initiation factor eIF4H facilitates loop-binding, repetitive RNA unwinding by the eIF4A DEAD-box helicase. *Nucleic Acids Res.*, **40**, 6199–6207.
20. Nielsen,K.H., Behrens,M.A., He,Y., Oliveira,C.L., Sottrup Jensen,L., Hoffmann,S.V., Pedersen,J.S. and Andersen,G.R. (2011) Synergistic activation of eIF4A by eIF4B and eIF4G. *Nucleic Acids Res.*, **15**, 67–75.
21. Rozovsky,N., Butterworth,A.C. and Moore,M.J. (2008) Interactions between eIF4AI and its accessory factors eIF4B and eIF4H. *RNA***14**, 2136–2148.
22. Bi,X., Ren,J. and Goss,D.J. (2000) Wheat germ translation initiation factor eIF4B affects eIF4A and eIFiso4F helicase activity by increasing the ATP binding affinity of eIF4A. *Biochemistry*, **39**, 5758–5765.
23. Berset,C., Trachsel,H. and Altmann,M. (1998) The TOR (target of rapamycin) signal transduction pathway regulates the stability of translation initiation factor eIF4G in the yeast saccharomyces cerevisiae. *Proc. Natl. Acad. Sci. U.S.A.*, **95**, 4264–4269.
24. Barbet,N.C., Schneider,U., Helliwell,S.B., Stansfield,I., Tuite,M.F. and Hall,M.N. (1996) TOR controls translation initiation and early G1 progression in yeast. *Mol. Biol. Cell*, **7**, 25–42.
25. Lindqvist,L. and Pelletier,J. (2009) Inhibitors of translation initiation as cancer therapeutics. *Future Med Chem*, **1**, 1709–1722.
26. von der Haar,T. and McCarthy,J.E. (2002) Intracellular translation initiation factor levels in *Saccharomyces cerevisiae* and their role in cap-complex function. *Mol. Microbiol.*, **46**, 531–544.
27. O'Leary,S.E., Petrov,A., Chen,J. and Puglisi,J.D. (2013) Dynamic recognition of the mRNA cap by *saccharomycescerevisiae* eIF4E. *Structure*, **21**, 2197–2207.
28. Hilbert,M., Kebbel,F., Gubaev,A. and Klostermeier,D. (2011) eIF4G stimulates the activity of the DEAD box protein eIF4A by a conformational guidance mechanism. *Nucleic Acids Res.*, **39**, 2260–2270.
29. Mitchell,S.F., Walker,S.E., Algire,M.A., Park,E.H., Hinnebusch,A.G. and Lorsch,J.R. (2010) The 5′-7-methylguanosine cap on eukaryotic mRNAs serves both to stimulate canonical translation initiation and to block an alternative pathway. *Mol. Cell*, **39**, 950–962.
30. Volpon,L., Culjkovic-Kraljacic,B., Sohn,H.S., Blanchet-Cohen,A., Osborne,M.J. and Borden,K.L.B. (2017) A biochemical framework for eIF4E-dependent mRNA export and nuclear recycling of the export machinery. *RNA*, **23**, 927–937.
31. Yourik,P., Aitken,C.E., Zhou,F., Gupta,N., Hinnebusch,A.G. and Lorsch,J.R. (2017) Yeast eIF4A enhances recruitment of mRNAs regardless of their structural complexity. *Elife*, **6**, e31476.
32. Oberer,M., Marintchev,A. and Wagner,G. (2005) Structural basis for the enhancement of eIF4A helicase activity by eIF4G. *Genes Dev.*, **19**, 2212–2223.
33. Volpon,L., Osborne,M.J. and Borden,K.L. (2006) NMR assignment of human eukaryotic translation initiation factor 4E (eIF4E) in its cap-free form. *J. Biomol. NMR*, **36**, 65.
34. Volpon,L., Osborne,M.J., Topisirovic,I., Siddiqui,N. and Borden,K.L. (2006) Cap-free structure of eIF4E suggests a basis for conformational regulation by its ligands. *EMBO J.*, **25**, 5138–5149.
35. Marintchev,A., Edmonds,K.A., Marintcheva,B., Hendrickson,E., Oberer,M., Suzuki,C., Herdy,B., Sonenberg,N. and Wagner,G. (2009) Topology and regulation of the human eIF4A/4G/4H helicase complex in translation initiation. *Cell*, **136**, 447–460.
36. Siddiqui,N., Tempel,W., Nedyalkova,L., Volpon,L., Wernimont,A.K., Osborne,M.J., Park,H.W. and Borden,K.L. (2012) Structural insights

into the allosteric effects of 4EBP1 on the eukaryotic translation initiation factor eIF4E. *J. Mol. Biol.*, **415**, 781–792.
37. Morino,S., Imataka,H., Svitkin,Y.V., Pestova,T.V. and Sonenberg,N. (2000) Eukaryotic translation initiation factor 4E (eIF4E) binding site and the middle one-third of eIF4GI constitute the core domain for cap-dependent translation, and the C-terminal one-third functions as a modulatory region. *Mol. Cell. Biol.*, **20**, 468–477.
38. Papadopoulos,E., Jenni,S., Kabha,E., Takrouri,K.J., Yi,T., Salvi,N., Luna,R.E., Gavathiotis,E., Mahalingam,P., Arthanari,H. *et al.* (2014) Structure of the eukaryotic translation initiation factor eIF4E in complex with 4EGI-1 reveals an allosteric mechanism for dissociating eIF4G. *Proc. Natl. Acad. Sci. U.S.A.*, **111**, E3187–E3195.
39. von der Haar,T., Oku,Y., Ptushkina,M., Moerke,N., Wagner,G., Gross,J.D. and McCarthy,J.E. (2006) Folding transitions during assembly of the eukaryotic mRNA cap-binding complex. *J. Mol. Biol.*, **356**, 982–992.
40. von Der Haar,T., Ball,P.D. and McCarthy,J.E. (2000) Stabilization of eukaryotic initiation factor 4E binding to the mRNA 5′-Cap by domains of eIF4G. *J. Biol. Chem.*, **275**, 30551–30555.
41. Yanagiya,A., Svitkin,Y.V., Shibata,S., Mikami,S., Imataka,H. and Sonenberg,N. (2008) Requirement of RNA-binding of mammalian eIF4GI for efficient interaction of eIF4E with mRNA cap. *Mol. Cell. Biol.*, **29**, 1661–1669.
42. Cetin,B., Song,G.J. and O'Leary,S.E. (2020) Heterogeneous dynamics of protein-RNA interactions across transcriptome-derived messenger RNA populations. *J. Am. Chem. Soc.*, **142**, 21249–21253.
43. Imataka,H. and Sonenberg,N. (1997) Human eukaryotic translation initiation factor 4G (eIF4G) possesses two separate and independent binding sites for eIF4A. *Mol. Cell. Biol.*, **17**, 6940–6947.
44. Dominguez,D., Altmann,M., Benz,J., Baumann,U. and Trachsel,H. (1999) Interaction of translation initiation factor eIF4G with eIF4A in the yeast *saccharomycescerevisiae*. *J. Biol. Chem.*, **274**, 26720–26726.
45. Korneeva,N.L., Lamphear,B.J., Hennigan,F.L., Merrick,W.C. and Rhoads,R.E. (2001) Characterization of the two eIF4A-binding sites on human eIF4G-1. *J. Biol. Chem.*, **276**, 2872–2879.
46. Korneeva,N.L., First,E.A., Benoit,C.A. and Rhoads,R.E. (2005) Interaction between the NH2-terminal domain of eIF4A and the central domain of eIF4G modulates RNA-stimulated ATPase activity. *J. Biol. Chem.*, **280**, 1872–1881.
47. Bellsolell,L., Cho-Park,P.F., Poulin,F., Sonenberg,N. and Burley,S.K. (2006) Two structurally atypical HEAT domains in the C-Terminal portion of human eIF4G support binding to eIF4A and mnk1. *Structure*, **14**, 913–923.
48. Berset,C., Zurbriggen,A., Djafarzadeh,S., Altmann,M. and Trachsel,H. (2003) RNA-binding activity of translation initiation factor eIF4G1 from *saccharomycescerevisiae*. *RNA*, **9**, 871–880.
49. Park,E.H., Walker,S.E., Lee,J.M., Rothenburg,S., Lorsch,J.R. and Hinnebusch,A.G. (2011) Multiple elements in the eIF4G1 N-terminus promote assembly of eIF4G1*PABP mRNPs *in vivo*. *EMBO J.*, **30**, 302–316.
50. Gulay,S., Gupta,N., Lorsch,J.R. and Hinnebusch,A.G. (2020) Distinct interactions of eIF4A and eIF4E with RNA helicase ded1 stimulate translation *in vivo*. *Elife*, **9**, e58243.
51. Andreou,A.Z., Harms,U. and Klostermeier,D. (2019) Single-stranded regions modulate conformational dynamics and ATPase activity of eIF4A to optimize 5′-UTR unwinding. *Nucleic Acids Res.*, **47**, 5260–5275.
52. Gao,Z., Putnam,A.A., Bowers,H.A., Guenther,U.P., Ye,X., Kindsfather,A., Hilliker,A.K. and Jankowsky,E. (2016) Coupling between the DEAD-box RNA helicases ded1p and eIF4A. *Elife*, **5**, e16408.
53. Park,E.H., Walker,S.E., Zhou,F., Lee,J.M., Rajagopal,V., Lorsch,J.R. and Hinnebusch,A.G. (2013) Yeast eukaryotic initiation factor (eIF) 4B enhances complex assembly between eIF4A and eIF4G *invivo*. *J. Biol. Chem.*, **288**, 2340–2354.
54. Ozes,A.R., Feoktistova,K., Avanzino,B.C. and Fraser,C.S. (2011) Duplex unwinding and ATPase activities of the DEAD-Box helicase eIF4A are coupled by eIF4G and eIF4B. *J. Mol. Biol.*, **412**, 674–687.
55. Rogers,G.W., Lima,W.F. Jr and Merrick,W.C. (2001) Further characterization of the helicase activity of eIF4A. Substrate specificity. *J. Biol. Chem.*, **276**, 12598–12608.
56. Lorsch,J.R. and Herschlag,D. (1998) The DEAD box protein eIF4A. 2. A cycle of nucleotide and RNA-dependent conformational changes. *Biochemistry*, **37**, 2194–2206.
57. Lorsch,J.R. and Herschlag,D. (1998) The DEAD box protein eIF4A. 1. A minimal kinetic and thermodynamic framework reveals coupled binding of RNA and nucleotide. *Biochemistry*, **37**, 2180–2193.
58. Fuchs,A.L., Neu,A. and Sprangers,R. (2016) A general method for rapid and cost-efficient large-scale production of 5′ capped RNA. *RNA*, **22**, 1454–1466.
59. Goessringer,M., Helmecke,D., Koehler,K., Schoen,A., Kirsebom,L.A., Bindereif,A and Hartmann,R.K. (2014) In: Hartmann,R.K., Bindereif,A., Schoen,A. and Westhof,E. (eds). *Handbook of RNA Biochemistry*. Wiley-VCH Verlag GmbH & Co. KGaA, pp. 3–28.
60. Adam,H. (1962) In: *Methoden der enzymatischen Analyse*. Bergmeyer, H.U.(Hrsg.), Verlag Chemie, Weinheim, pp. 573–577.
61. Andreou,A.Z. and Klostermeier,D. (2012) Conformational changes of DEAD-Box helicases monitored by single molecule fluorescence resonance energy transfer. *Methods Enzymol.*, **511**, 75–109.
62. Rogers,G.W., Richter,N.J. Jr and Merrick,W.C. (1999) Biochemical and kinetic characterization of the RNA helicase activity of eukaryotic initiation factor 4A. *J. Biol. Chem.*, **274**, 12236–12244.
63. Kaye,N.M., Emmett,K.J., Merrick,W.C. and Jankowsky,E. (2009) Intrinsic RNA binding by the eukaryotic initiation factor 4F depends on a minimal RNA length, but not on the m7G cap. *J. Biol. Chem.*, **284**, 17742–17750.
64. Pause,A., Methot,N., Svitkin,Y., Merrick,W.C. and Sonenberg,N. (1994) Dominant negative mutants of mammalian translation initiation factor eIF-4A define a critical role for eIF-4F in cap-dependent and cap-independent initiation of translation. *EMBO J.*, **13**, 1205–1215.
65. Hong,H.J., Guevara,M.G., Lin,E. and O'Leary,S.E. (2021) Single-Molecule dynamics of SARS-CoV-2 5′ cap recognition by human eIF4F. bioRxiv doi: https://doi.org/10.1101/2021.05.26.445185, 27 May 2021, preprint: not peer reviewed.
66. Wang,H., Sun,L., Gaba,A. and Qu,X. (2020) An *in vitro* single-molecule assay for eukaryotic cap-dependent translation initiation kinetics. *Nucleic Acids Res.*, **48**, e6.
67. Duss,O., Stepanyuk,G.A., Grot,A., O'Leary,S.E., Puglisi,J.D. and Williamson,J.R. (2018) Real-time assembly of ribonucleoprotein complexes on nascent RNA transcripts. *Nat. Commun.*, **9**, 5087.